# PRECIPITATION AND COLD AIR PRODUCTION IN MESOSCALE THUNDERSTORM SYSTEMS [1]

*By Tetsuya Fujita*

The University of Chicago

(Manuscript received 3 November 1958)

ABSTRACT

This paper presents a proposed mechanism of cold air production associated with precipitation. A dome of cold air is produced by the evaporation of raindrops falling beneath the cloud base. A quantitative relationship between the evaporated rain and the produced excess mass of cold air was obtained, which showed that the mass is directly proportional to the evaporation. The coefficient of proportionality is a dimensionless number which varies between 0 and 1 depending on the temperature lapse rate originally existing beneath the cloud base. Results of mesoanalyses of squall lines and thunderstorms were used to estimate the actual amount of evaporation. The mass ratio of evaporated rain to the surface rain was found to increase with the height of the cloud base, reaching 1.0 at a cloud base of 9000 ft. In-cloud evaporation obtained by Braham (1952) showed a very good agreement with the values obtained in this study.

## 1. Introduction

It is well known that the surface pressure rises and oscillates appreciably when thunderstorms pass over a station. Suckstorff (1935) postulated that the cold air contributing to the rise is produced by precipitation. The published results of the Thunderstorm Project (1949) revealed the fact that the downdrafts descending through the storm clouds are the source of the air forming the cold dome over the ground. Byers (1951) pointed out and explained two important features of thunderstorm pressure traces, the 'dome' and the 'nose'.

In case of squall-line thunderstorms, the pressure field is characterized by a line of tight pressure gradient at the leading edge of the line and by the pressure dome associated with the individual cells. Williams (1948) made synoptic analyses of line thunderstorms which passed over the area of the Thunderstorm Project network and revealed the features of the traveling pressure gradient. However, it was not clear that the pressure gradient on the progressing side of the squall line was the result of individual storms.

One step toward the medium-scale, or mesoscale, pressure analysis was undertaken by Tepper (1950), leading him to propose a mechanism of a 'pressure-jump line' caused by a gravitational wave. Further studies made by him (1952) confirmed the existence of pressure-jump waves propagating as far as several hundred miles without affecting the surface temperature field, as well as the fact that the velocity of the line usually differs appreciably from the upper wind velocity at any level up to the tropopause. If the excess pressure (actual pressure less undisturbed pressure) to the rear of the line were integrated over the area, it would not change with time to an appreciable degree.

Recent work on mesoanalyses of various systems by Fujita, Newstein, and Tepper (1956) and by Fujita and Brown (1958) proved the frequent appearance of a mesoscale dome-type pressure disturbance accompanied by squall-line thunderstorms. This type of disturbance develops in a small area of early activity of the thunderstorms and grows into a mesoscale system, or mesosystem, in several hours. The boundary of the system is defined by the edge of the pressure disturbance. When the associated radar echoes are essentially stationary, the pressure rises all around the boundary; however, if the echo velocity is comparatively high, the rise is significant only on the downwind side of the upper flow. This author (1955) has designated the mesosystem boundary accompanied by the rise in pressure as the 'pressure-surge line.' In some portion of the pressure-surge line, the amount, rate, and duration of the rise usually are large enough to satisfy the definition of 'pressure jump' established by the U. S. Weather Bureau (1956).

Fig. 1 shows an example of a line, running diagonally through the southern half of the area, which was not accompanied by thunderstorm activity and therefore could be explained as a gravitational wave of the type described by Tepper. In the northern half of the area, there is a pressure-surge line serving as the boundary of a mesosystem. The latter is by far the most common type of pressure-surge or pressure-jump line. It is accompanied by vigorous thunderstorm activity and a pronounced mesoscale high-pressure area.

[1] The research reported in this paper has been sponsored by the U. S. Weather Bureau, under contract Cwb 9321.

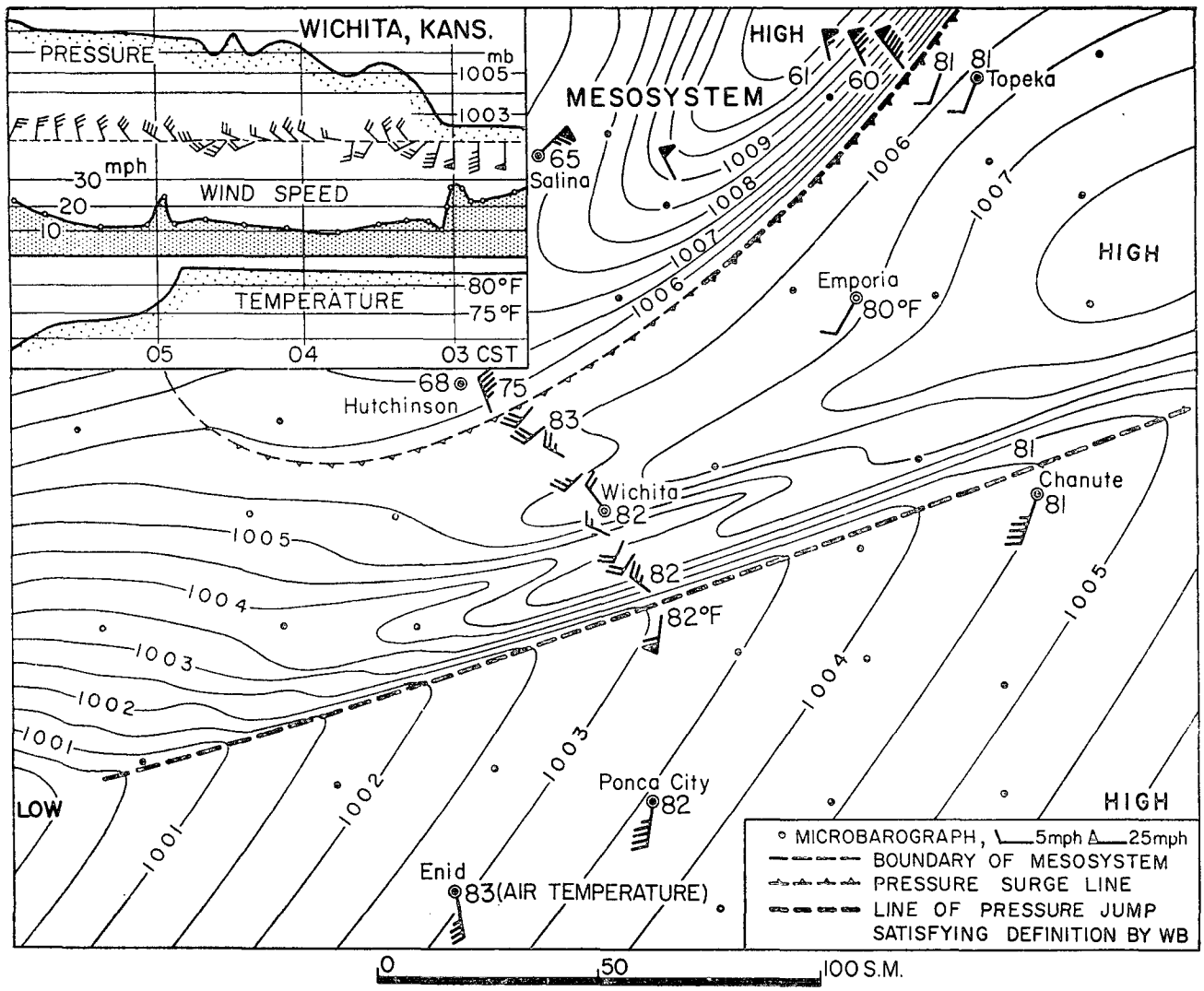


FIG. 1. Mesoanalysis chart for 0400 CST 25 June 1953 covering the area of the U. S. Weather Bureau Severe Local Storms Kansas-Oklahoma Network.

## 2. Vertical structure of cold dome

In order to clarify the vertical structure of the cellular-scale cold dome beneath the thunderstorm, fig. 2 was made by using the flight and surface data obtained by the Thunderstorm Project. In the lower sections, the time-adjusted surface charts appear on which is plotted the station weather occurring at the time when the project airplane was flying in a particular direction relative to the station. In each case, the direction perpendicular to the average orientation of the flight path was chosen. Therefore, the temperature profile obtained from the isotherms in the time-adjusted surface chart gives the surface cooling occurring directly beneath the airplane traversing the storm.

It will be found in the upper section of the charts that the 5000-ft temperature is rather uniform in comparison with the tremendous drop in temperature at the surface.

We next see the temperature field of the mesoscale cold dome. The selected level upper-air composite charts in fig. 3, analyzed by the author (1957), reveal the vertical structure of the dome. The temperature difference between the dome and environment atmosphere is pronounced only at the lowest levels and becomes insignificant at 4000 ft above the surface.

It is of interest to find that the mesoscale cold dome, covering an area several hundred times larger than that of the cellular dome, likewise extends up to only several thousand feet above the ground.

The purpose of this paper is to evaluate quantitatively the effect of precipitation upon the production of a pressure dome. In the actual case, however, the pressure nose defined by the Thunderstorm Project as being

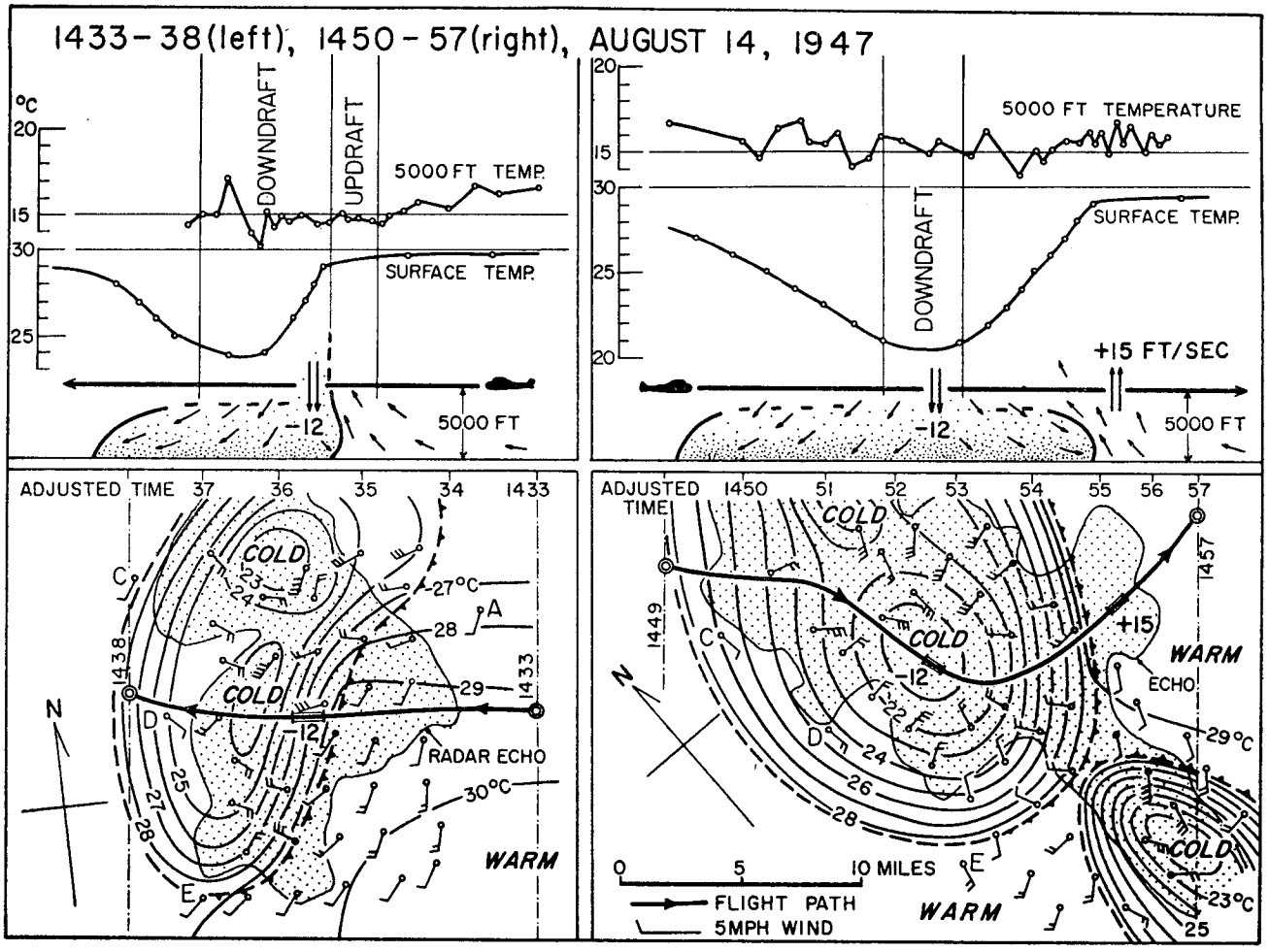


FIG. 2. Time-adjusted charts of Thunderstorm Project network area. Original data used for this analysis were taken from THE THUNDERSTORM, pp. 199–234.

1. a rate of pressure rise of 0.02 in per 5 min or more,
2. a total rise equal to or greater than 0.02 in, and
3. a pressure fall of at least 0.01 in within the 10 min following the maximum pressure associated with the pressure rise

appears somewhat like an additional hump superimposed on the pressure dome. Because of the fact that a nose is seen directly under an active thunderstorm cell, the pressure rise is considered to be a result of the vertical motion during a thunderstorm. A number of meteorologists, notably Levine (1942) and Schaffer (1947) estimated the amount of pressure change due to vertical motion.

The vertical velocities inside mesoscale pressure domes were computed by Fujita (1959). The results revealed that the vertical motion reaching up to 3.0 ft per sec is not large enough to cause an appreciable nonhydrostatic pressure rise.

### 3. Excess pressure and surface rain

The pressure field of a typical mesosystem with a horizontal dimension of about 150 × 200 mi is presented in fig. 4. The isobars of excess pressure indicated by the heavy contours were obtained graphically by subtracting the undisturbed pressure field from the actual field. The term 'undisturbed' is used, in this case, as meaning 'not disturbed by the cold dome.' For an exact definition, see reference (Fujita, 1955). The dynamics of the pressure rise will now be examined.

The latent heat released inside the updraft gives rise to the expansion of the atmosphere above the cloud base, resulting in a decrease of hydrostatic pressure over an area much larger than that of the mesosystem. This effect appears on a microbarograph trace as a rather rapid pressure drop preceding the pressure surge. Seen in the mesoanalysis chart are the concave isobars of undisturbed pressure.

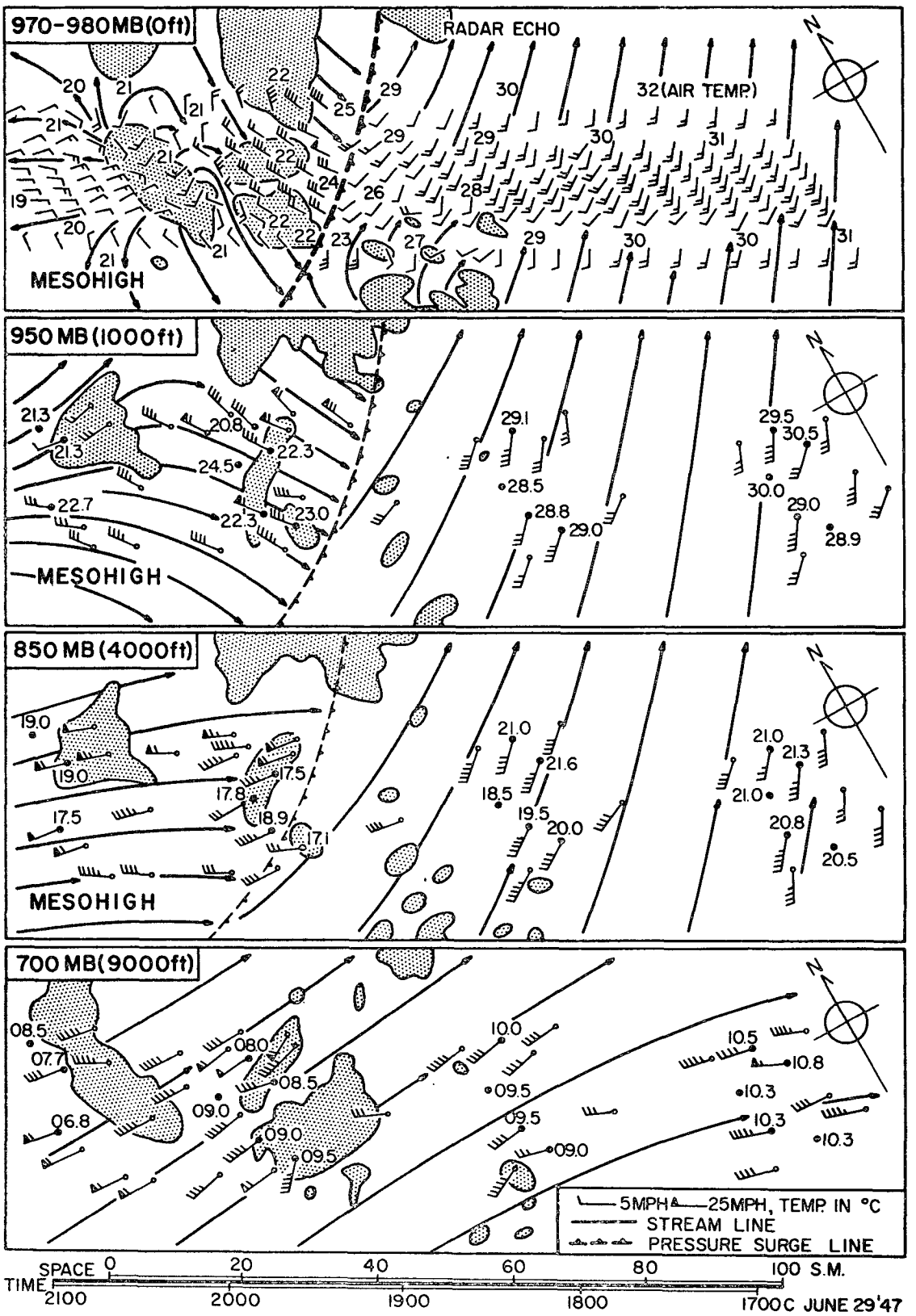


FIG. 3. Composite surface and upper-air charts of the squall-line mesosystem which passed over the Thunderstorm Project, Ohio area on 29 June 1947.

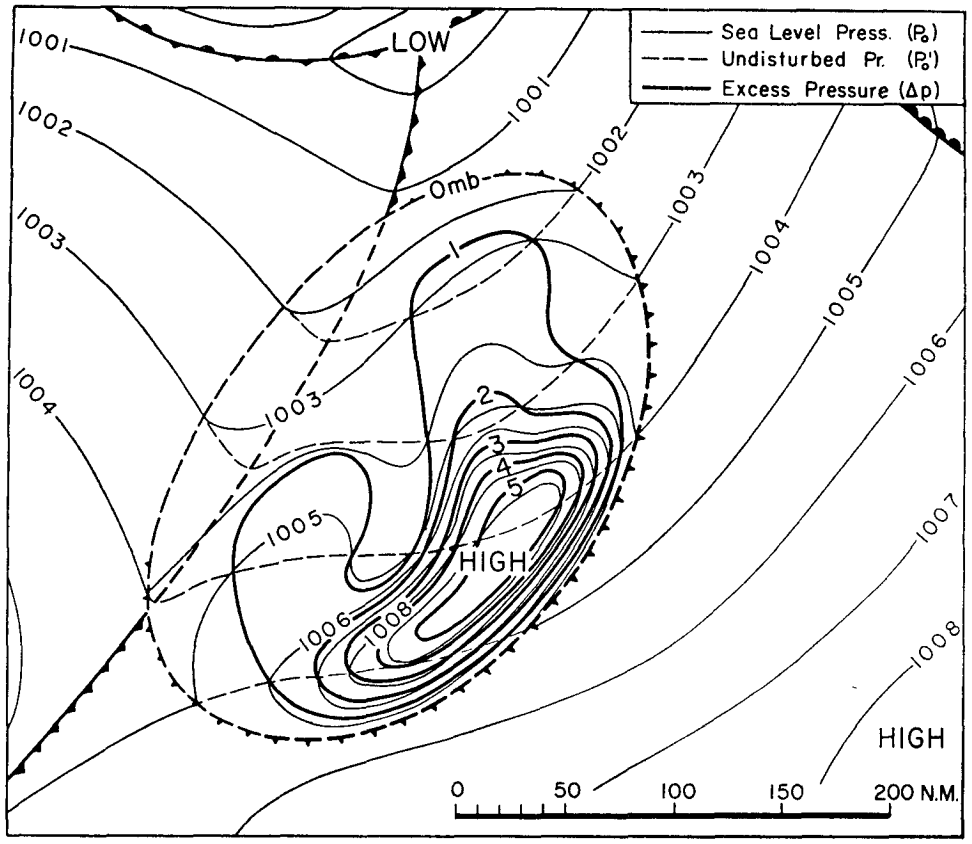


FIG. 4. An example of the excess pressure field of the squall-line mesosystem of 4 June 1953. Isobars of excess pressure were obtained graphically by connecting the successive intersections of isobars of sea-level and undisturbed pressure.

Let $P_0$ and $P_0'$ be the actual and undisturbed surface pressure, then the excess pressure and excess mass are expressed, respectively, by

$$\Delta p = P_0 - P_0' \quad \text{and} \quad \Delta m = \Delta p/g.$$

The total excess mass associated with the dome is defined by

$$\Delta M = \int_s \Delta m dS, \tag{1}$$

where $S$ is the area covered by the dome.

Results of areal integrations made for various squall-line mesosystems revealed that the value of $\Delta M$ was negligibly small when the system first appeared; then it increased with time for several hours until the precipitation inside the boundary of the system became light and widely scattered.

Assuming that the precipitation has something to do with the cold air production, the time-integrated surface rain,

$$r_s = \int_0^t (\text{rain})\, dt,$$

was again integrated by area. Thus the total surface rain,

$$R_s = \int_s r_s dS, \tag{2}$$

was obtained.

Fig. 5 shows the relationship between $\Delta M$ and $R_s$ for several systems occurring over the Great Plains. It is evident that $\Delta M$ increases approximately in proportion to $R_s$ in the development stage of the system. The slope of the curves given roughly by the ratio $\Delta M/R_s$ varies considerably with each system.

The geographic location of the systems under discussion is given in fig. 6. The isochrones of progress of the system boundary indicate that Systems I and II moved east-northeast, while the others over the Texas-Oklahoma area simply spread out. The distribution of the ratio $\Delta M/R_s$ is found to be extremely large for the particular system over the Texas Panhandle where the base of associated convective clouds was very high. Over the Mississippi and Ohio Valleys, the height of the cloud base was 4000 to 5000 ft. The system that developed there showed a ratio between 1.3 and 1.9. Of great importance is the finding that the cellular system over the area of the Thunderstorm Project, Ohio, is characterized by the ratio 1.4, suited to a mesoscale system which might develop in that area.

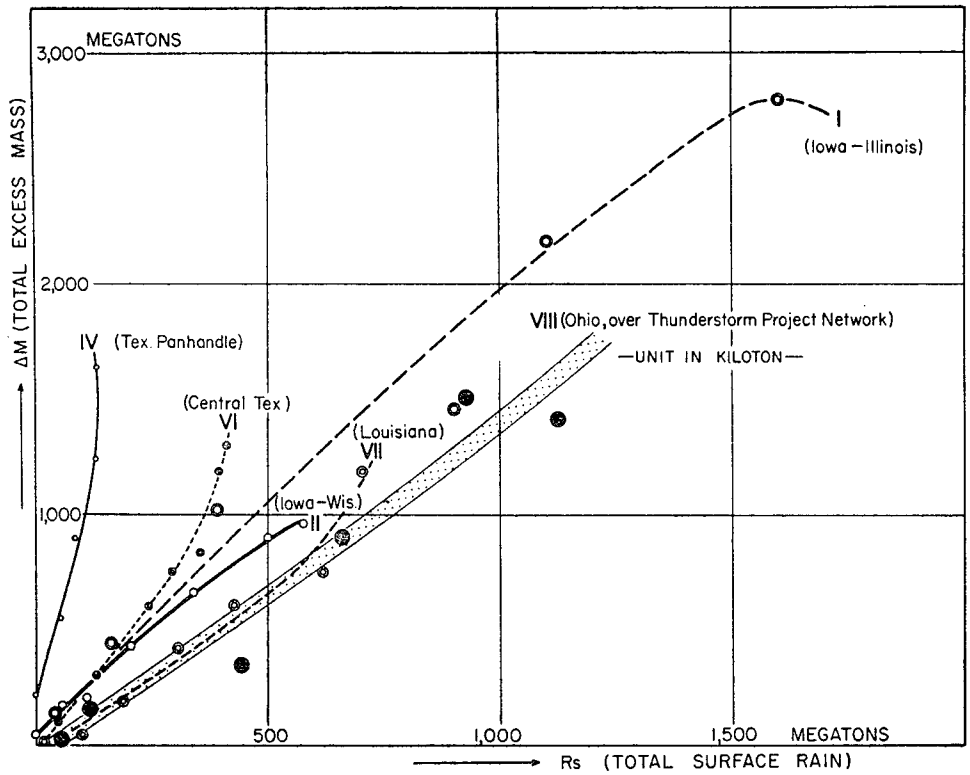


FIG. 5. The increase in total excess mass of squall-line mesosystems as a function of total surface rain. Both $\Delta M$ and $R_s$ of Systems I–VII were integrated for one-hour intervals. System VIII over the Thunderstorm Project area was so small that 10-min values of $\Delta M$ and $R_s$ were obtained in kilotons.

A mesoscale dome, therefore, is considered to be a group of cellular domes organized into a much larger system. For a given cloud base, the ratio of $\Delta M$ to $R_s$ appears to be more or less the same whether from a single cell or from an entire mesoscale system.

## 4. Subsidence of the cold dome

The characteristics of mesoscale cold domes discussed in the previous chapters may be summarized as follows:

1. The total excess mass of the cold dome in its development stage increases in proportion to the total surface rain which has fallen inside the system boundary.

2. The proportionality constant increases with the height of the convective cloud base.

3. The temperature difference of air inside and outside the dome is large at the surface and becomes less with height.

The research of the Thunderstorm Project revealed that the downdraft is not always saturated but that the moist-adiabatic process is roughly maintained during the descent as long as sufficient raindrops remain inside. Petterssen (1956) emphasized the conservation of potential wet-bulb temperature of the downdraft whether saturated or not. Similar statements have been made by many others suggesting that the downdraft, as a first approximation, can be assumed to descend moist-adiabatically.

Fig. 7 indicates the schematic temperature distribution inside the downdraft when it first touched the surface. The temperature of a parcell of environment air ascending dry-adiabatically from the ground is shown by the dry-adiabat U-A. It is well known that the in-cloud downdraft is colder than the updraft in its mature stage and that the downdraft is characterized by the pressure nose beneath the active cell. Above the dome, however, the temperature field above the cloud base is not so dependent upon the drafts (see fig. 2), so that we may assume the stippled triangular area UAD as accounting for the excess pressure on the ground.

Using the hydrostatic assumption, we denote the excess pressure as

$$\Delta p \doteqdot \rho_0 \int_{P_0}^{P_b} R\Delta T d(\ln p), \qquad (3)$$

where $\Delta T$ is the difference in environment and downdraft temperature; $\rho_0$, the surface air density; $P_b$ and $P_0$, the pressures at the cloud base and at the ground, respectively.

The vertical distribution of in-dome temperature,

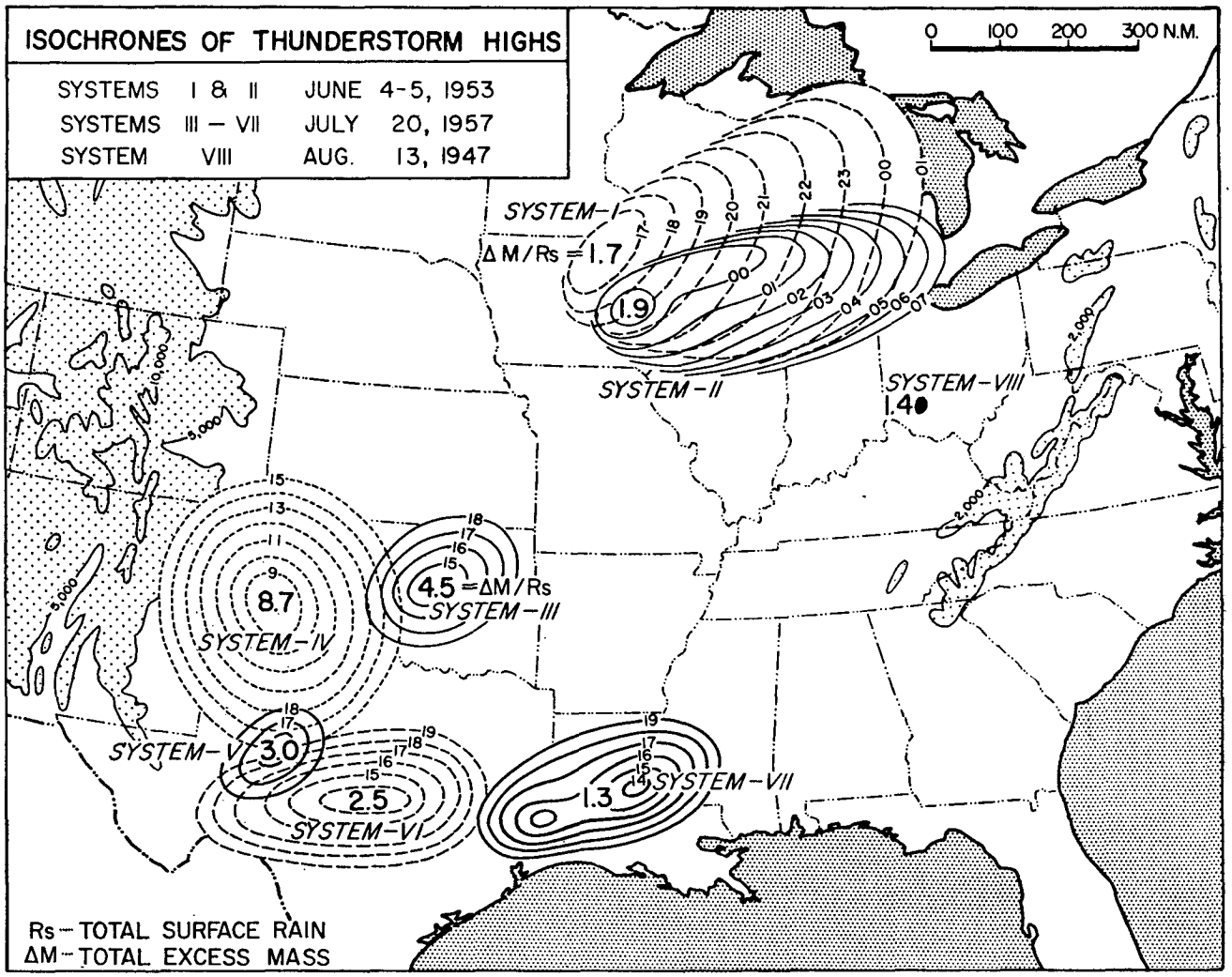


FIG. 6. Geographical location and horizontal dimensions of eight squall-line mesosystems, which are indicated by the pressure-surge isochrones drawn for one-hour intervals.

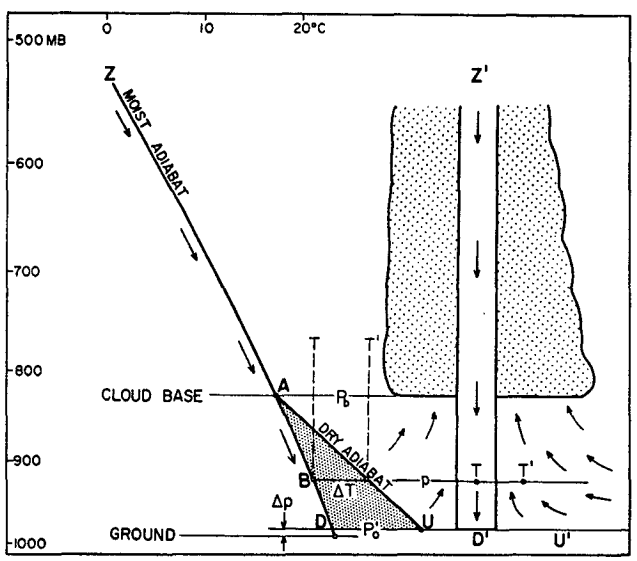


FIG. 7. Schematic diagram showing the cooling produced by in-draft evaporation of raindrops.

represented by a moist-adiabat when the dome is produced, changes rapidly due to subsidence (see fig. 8). If the dome does not contain water droplets, a dry-adiabatic subsidence of the dome takes place. Accordingly, the change of dry-bulb and dew-point temperature will be given by the dry-adiabats and constant mixing-ratio lines, respectively. When the gust is strong, an inversion surface appears at the top of the turbulence layer as shown in the figure. By the time the initial height of the dome H drops down to H′, the excess surface pressure, which is proportional to the area UGFE, decreases appreciably. In the meantime, the area covered by the dome increases.

The next problem is to compute the change in excess mass caused by the subsidence of the dome. Using the symbols shown in fig. 9, the excess pressure due to the volume element HIJK is given by

$$\delta\Delta p = \rho_0 R(T - T_c)\frac{\delta p}{p} \qquad (4)$$

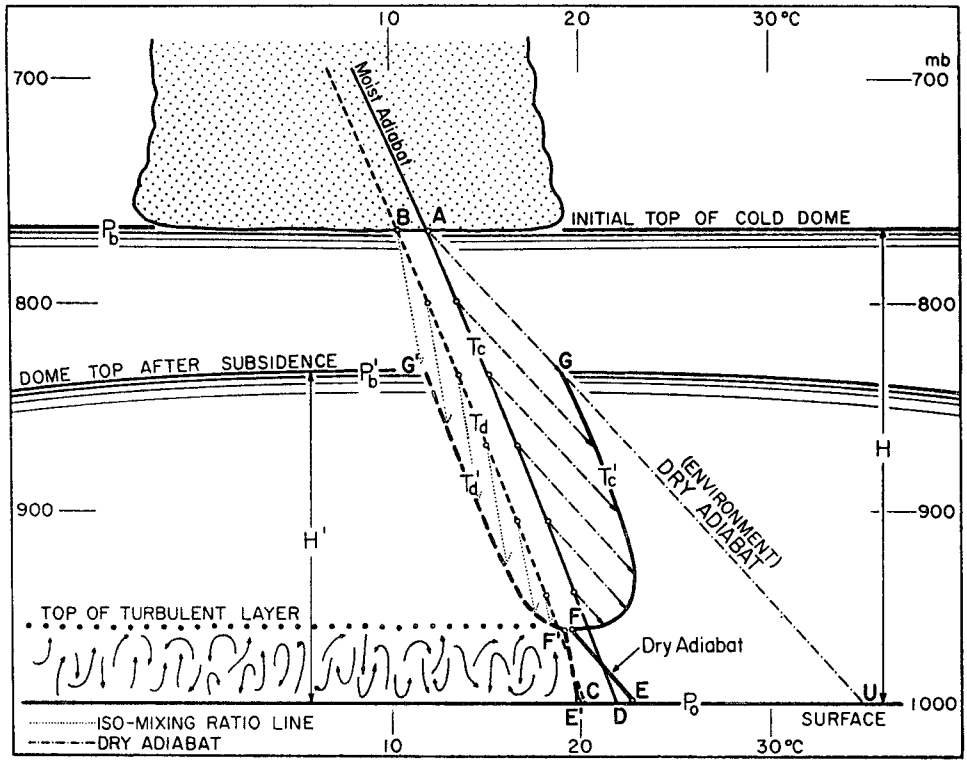


FIG. 8. Change in vertical distribution of dry- and wet-bulb temperature due to the subsidence of a cold dome. The initial relative humidity inside the downdraft was assumed to be 90 per cent.

where $\rho_0$ is the surface air density. After the subsidence, the element HIJK changes into LMNO which will exert surface excess pressure

$$\delta\Delta p' = \rho_0 R(T' - T_c') \frac{\delta p'}{p'}. \tag{5}$$

The total excess pressure, the excess pressure integrated over the surface directly under the volume elements, before and after subsidence is

$$S\delta\Delta p \quad \text{and} \quad S'\delta\Delta p',$$

respectively.

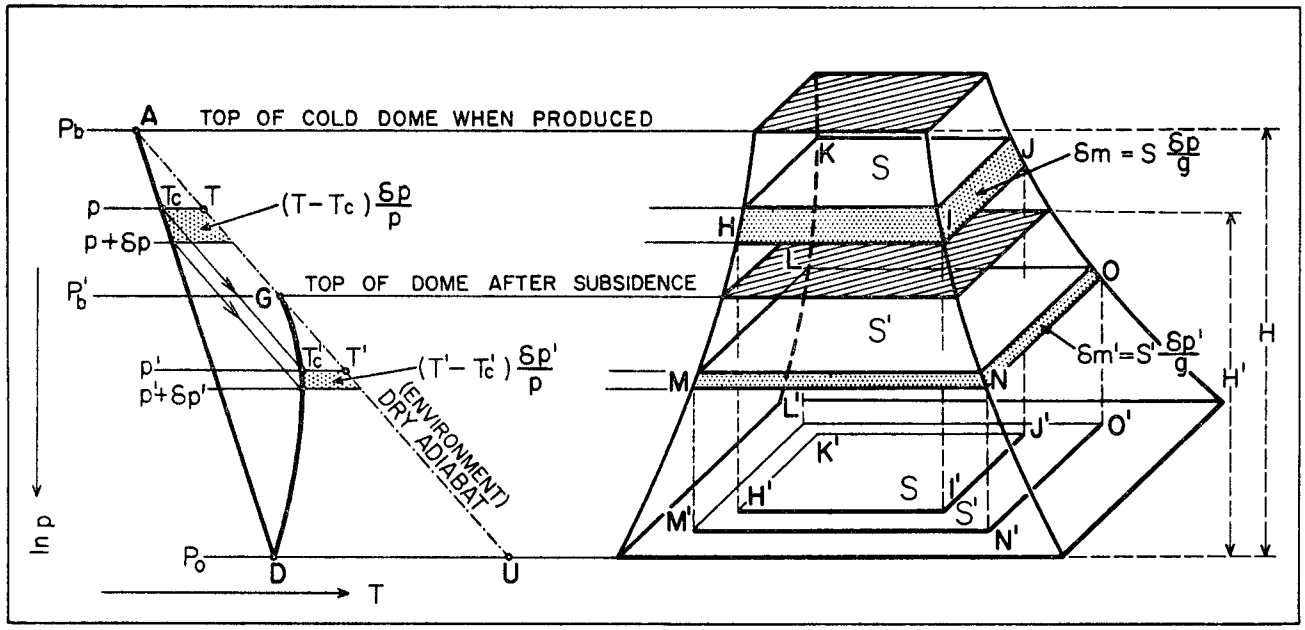


FIG. 9. Computation of the change in total excess mass assumed to be caused by subsidence of a cold dome.

Taking the ratio of the total excess masses defined by formula (1), we have

$$\frac{\delta\Delta M'}{\delta\Delta M} = \frac{S'\delta\Delta p'/g}{S\delta\Delta p/g} = \frac{S'(T' - T_c')\delta p'}{S(T - T_c)\delta p}\cdot\frac{p}{p'}. \quad (6)$$

Using the relations,

$$S'\delta p' = S\delta p = g\delta m \quad \text{(mass conservation)}$$

and

$$T'p'^{-k} = Tp^{-k}, \quad T_c'p'^{-k} = T_cp^{-k} \quad \text{(dry-adiabatic change)},$$

we reduce the ratio to

$$\frac{\delta\Delta M'}{\delta\Delta M} = \frac{S'}{S}\frac{p^{-k}}{p'^{-k}}\frac{S}{S'}\frac{p}{p'} = \left(\frac{p}{p'}\right)^{1-k}. \quad (7)$$

This formula denotes the change in excess mass of individual volume elements inside the subsiding dome. Thus, the ratio of total excess mass can be written as

$$\frac{\Delta M'}{\Delta M} = \frac{S\delta\Delta M'}{S\delta\Delta M} = \left(\frac{\bar{P}}{\bar{P}'}\right)^{1-k} \quad (8)$$

where $\bar{P}$ and $\bar{P}'$ are the mean pressure of the cold air column before and after the subsidence. Assuming that this mean pressure is equal to the pressure at the center of gravity of the semi-triangular areas, ADU and GDU, we express this approximately as

$$\bar{P}' \doteqdot \tfrac{1}{3}(2P_0 + P_b') \quad \text{and} \quad \bar{P} \doteqdot \tfrac{1}{3}(2P_0 + P_b)$$

where $P_b$ and $P_b'$ are the pressure at the dome top before and after the subsidence. Finally, the change in the total excess pressure due to the subsidence is given by

$$\frac{\Delta M'}{\Delta M} = \left(\frac{2P_0 + P_b}{2P_0 + P_b'}\right)^{1-k}. \quad (9)$$

Table 1 shows how much the total excess mass decreases as the dome top subsides.

TABLE 1. The ratio $\Delta M'/\Delta M$ as a function of $P_b$, the initial pressure, and $P_b'$, the final pressure, at the dome top.

| $P_b'$ | $P_b$=650 | $P_b$=700 | $P_b$=800 | $P_b$=900-mb |
|---|---|---|---|---|
| 650-mb | 1.00 | | | |
| 700 | 0.98 | 1.00 | | |
| 800 | 0.95 | 0.96 | 1.00 | |
| 900 | 0.94 | 0.95 | 0.96 | 1.00 |
| 1000 | 0.92 | 0.93 | 0.95 | 0.96 |

From the table, it is evident that as much as 92 per cent of the initial value of the total excess mass of the cold dome is conserved, even if the dome top subsides from the 650- to 1000-mb level, which would be an extreme case. This fact permits us to assume that the mass remains unchanged through the subsidence process. Accordingly, the areal integration of excess mass inside the mesosystem boundary gives the total amount of excess mass of cold air which has been produced up to the time of the integration.

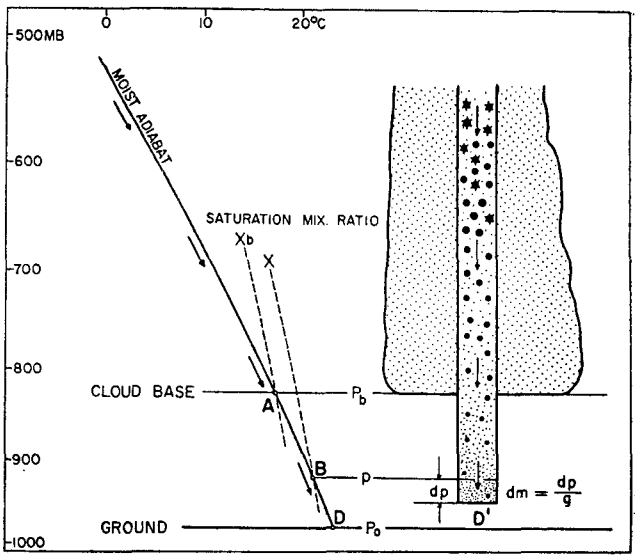


FIG. 10. Schematic diagram showing the increase in the mixing ratio of the in-draft air parcel which maintains saturation during the descent.

## 5. Evaporation of raindrops in downdraft

The air forming the downdraft is not always saturated, because the rate of evaporation is usually too slow to maintain 100 per cent relative humidity. In the following computation, however, it is assumed that the air parcel remains saturated during its descent.

The downdraft in its stage of development is illustrated in fig. 10. The mass of raindrops which evaporates inside the unit mass of descending air is approximately equal to the increase in mixing ratio. Let $X_b$ and $X$ be the saturation mixing ratio in $g/g$ of a descending air parcel at the cloud base and at the level of pressure $p$, respectively. We express the amount of evaporation by the integration

$$x - x_b = \int_{P_b(\theta e)}^{p(\theta e)} \left(\frac{\partial x}{\partial p}\right)_{\theta e} dp \quad (10)$$

where $P_b$ is the pressure at the cloud base.

The total amount of evaporation inside the column of downdraft, having a unit cross-sectional area, is obtained by integrating the above formula multiplied by $dm = dp/g$, the mass of the volume element. Thus, we have

$$r_e = (x - x_b)dm = \int_{P_bk(\theta e)}^{P_0(\theta e)} \frac{1}{g}\int_{P_b(\theta e)}^{p(\theta e)} \left(\frac{\partial x}{\partial p}\right)_{\theta e} dpdp \quad (11)$$

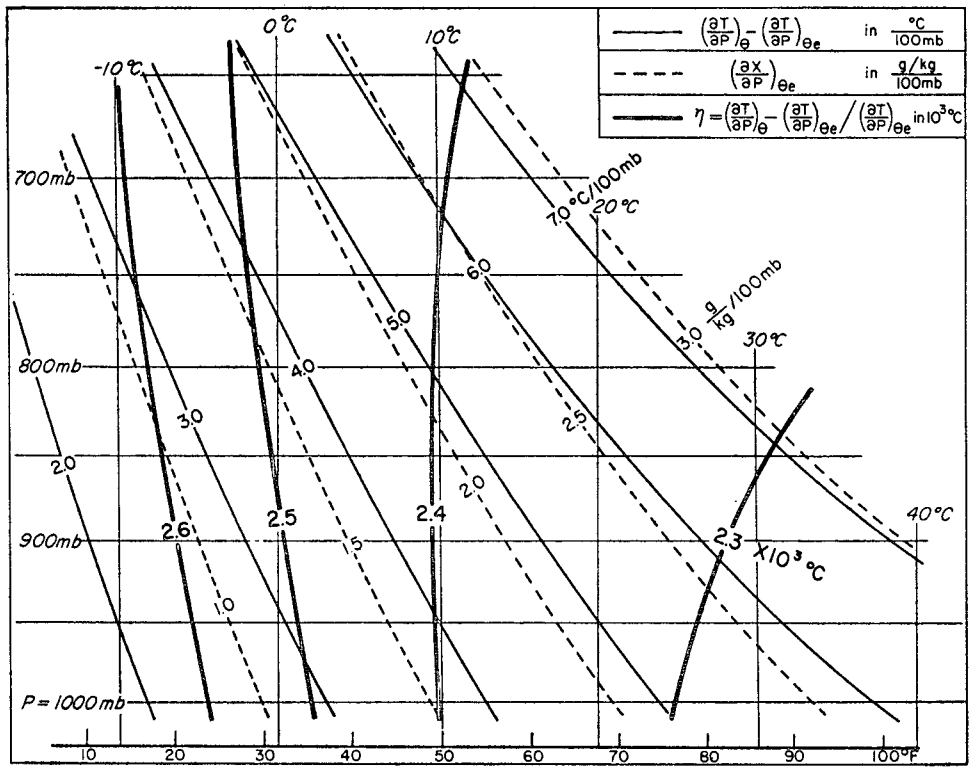


FIG. 11. Iso-lines of $(\partial T/\partial p)_\theta - (\partial T/\partial p)_{\theta e}$, $(\partial X/\partial p)_{\theta e}$ and their ratio drawn on an adiabatic chart.

where $P_0$ is the surface pressure, and $r_e$ the amount of evaporation inside the unit air column between the cloud base and the ground.

### 6. Excess mass due to precipitation cooling

Assuming the temperature lapse rate inside the cold dome to be moist-adiabatic, the difference in pressure inside and outside the downdraft is expressed by

$$\Delta p \doteqdot \rho_0 \Delta\Phi = \rho_0 R \int_{P_b}^{P_0} \Delta T d(\ln p) \qquad (12)$$

where $R$ is the specific gas constant; $\rho_0$, the surface air density; $\Delta T$, the temperature difference between dry and moist adiabats. In order to perform this integration with respect to pressure, we introduce the mean pressure $P$ satisfying the identity

$$\int_{P_b}^{P} \Delta T d(\ln p) \equiv \frac{1}{\bar{\bar{P}}} \int_{P_b}^{P_0} \Delta T dp. \qquad (13)$$

If the distribution of $\Delta T$ is given, $\bar{\bar{P}}$ can be obtained as a function of $P_0$ and $P_b$. As shown in fig. 7, $\Delta T$ is roughly proportional to the difference in logarithms of pressure at the cloud base and at an arbitrary level. Putting the proportional relationship

$$\Delta T \doteqdot k(\ln p - \ln P_b) \qquad (14)$$

into formula (13), we obtain the mean pressure

$$\bar{\bar{P}} = P_0(1 - \tfrac{1}{3}x - \tfrac{1}{6}x^2 \cdots)$$

where $x = (P_0 - P_b)/P_0$. If $x = 0.35$, corresponding to $P_0 = 1000$ mb and $P_b = 650$ mb, the third term in the parenthesis is less than 0.02. Neglecting, therefore, the terms of higher order, we have

$$\bar{\bar{P}} = P_0 \frac{4P_b - P_0}{3P_b}. \qquad (15)$$

Let the dry- and moist-adiabatic lapse rate be

$$\Gamma_d \left(\frac{\partial T}{\partial p}\right)_\theta \quad \text{and} \quad \Gamma_m = \left(\frac{\partial T}{\partial p}\right)_{\theta e}$$

respectively; therefore, the temperature difference of dry and moist adiabats meeting at the cloud base can be written as

$$\Delta T = \int_{P_b(\theta)}^{p(\theta)} \Gamma_d dp - \int_{P_b(\theta e)}^{p(\theta e)} \Gamma_m dp. \qquad (16)$$

The equation of dry-adabatic change,

$$T\left(\frac{P_0}{p}\right)^{(\gamma-1)/\gamma} = \text{const.},$$

is used to estimate the difference which would appear if $\Gamma_d$ is intetgraed along the moist adiabat. Then the following approximation is adequate within the range

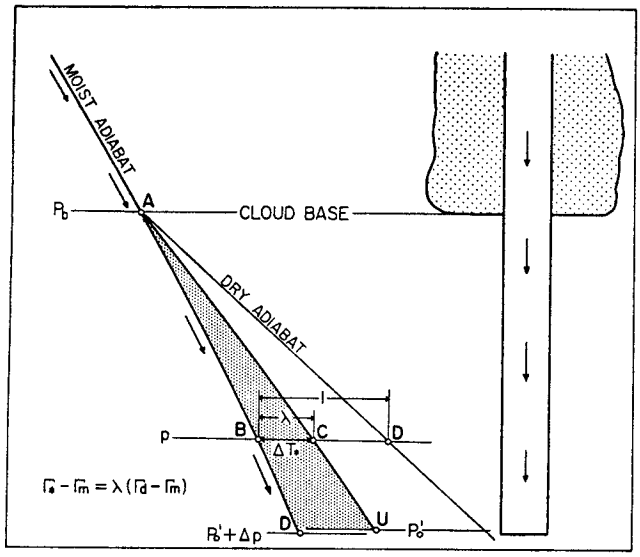


FIG. 12. Computation of excess pressure produced by the saturated downdraft descending through the environment atmosphere which is characterized by an arbitrary temperature lapse rate.

of pressure and temperature of the atmosphere beneath the cloud base:

$$\int \Gamma_d dp = (1.00 \sim 1.03) \int_{\theta e} \Gamma_d dp \doteqdot \int_{\theta e} \Gamma_d dp. \quad (17)$$

Thus, the combination of the equations (12), (16), and (17) permits us to compute the excess pressure by

$$\Delta p = \rho_0 R \frac{1}{\bar{P}} \int_{P_c}^{P_0} \int_{P_c}^{p} \left[ \left( \frac{\partial T}{\partial p} \right)_\theta - \left( \frac{\partial T}{\partial p} \right)_{\theta e} \right] dp dp. \quad (18)$$

In order to reveal the relationship between equations (11) and (18), we should know the values of

$$(\Gamma_d - \Gamma_m) \quad \text{and} \quad \left( \frac{\partial x}{\partial p} \right)_{\theta e},$$

each of which is given as a function of $p$ and $T$, respectively. The result of this computation appears in fig. 11. The figure reveals that the iso-lines of these two functions are alike. It follows naturally to take the ratio

$$\eta = (\Gamma_d - \Gamma_m) \Big/ \left( \frac{\partial x}{\partial p} \right)_{\theta e}. \quad (19)$$

The heavy iso-lines showing $\eta$ make it clear that this ratio, within the pressure and temperature range under discussion, is $(2.4 \pm 0.2)$, $\times 10^3$C and is nearly a constant.

With the use of equation (19), we now express the excess pressure (equation 18) by the evaporated rain (equation 11). Thus, we obtain the important formula

$$\Delta p = \rho_0 R \frac{\eta}{P} r_e.$$

Combining this equation with that of the mean pressure given by equation (15) and the equation of an ideal gas, we have

$$\Delta p = g \frac{\eta}{T_0} \left( \frac{3P_b}{4P_b - P_0} \right) r_e$$

or

$$\Delta m = \frac{\Delta p}{g} = \frac{\eta}{T_0} \left( \frac{3P_b}{4P_b - P_0} \right) r_e \quad (20)$$

where $T_0$ is the surface temperature. Using the numerical values,

$$\eta = (2.4 \pm 0.2) \times 10^3\text{C}, \quad T_0 = (1.00 \pm 0.07) \times 290\text{C},$$
$$3P_b/(4P_b - p_0) = 1.0 \pm 0.1,$$

we obtain

$$\Delta m \doteqdot 9 r_e, \quad \text{or} \quad \Delta p \doteqdot 9 g r_e \quad (21)$$

or, finally,

$$\Delta M \doteqdot 9 R_e. \quad (22)$$

This indicates that the total excess mass of cold air is nine times larger than the mass of raindrops evaporated inside the downdraft beneath the cloud base.

## 7. Generalization of cold air production formula

The preceding discussion has been based on the assumption that the excess mass of cold air is produced inside the downdraft surrounded by the dry-adiabatic environment atmosphere. In this section, we discuss the situation (see fig. 12) in which the downdraft replaces the underlying atmosphere with the temperature lapse rate, $\Gamma^*$, defined by

$$\Gamma^* - \Gamma_m = \lambda(\Gamma_d - \Gamma_m) \quad (23)$$

where $\lambda$ is a parameter to give an arbitrary lapse rate.

In this generalized case, we obtain the excess pressure from equations (12), (15), and (18), with the result

$$\Delta p = 9 g \lambda r_e. \quad (24)$$

Integrating both sides over the entire area of the dome, we have

$$\Delta M = 9 \lambda R_e. \quad (25)$$

TABLE 2. Approximate values of $\lambda$ associated with various types of rain.

| Type of rain | | Pressure system produced |
|---|---|---|
| Thundershower | $1-\frac{3}{4}$ | Cellular or mesoscale pressure dome |
| Shower | $\frac{3}{4}-\frac{1}{2}$ | Pressure pulsation or oscillation |
| Warm-frontal rain | $\frac{1}{2}-\frac{1}{4}$ | Insignificant pressure rise |
| In-cloud rain | $\frac{1}{4}-0$ | Pressure nose associated with melting snow or hail |

As shown in the table, $\lambda$ is very close to 1.00 for thunderstorms which occur over the heated continent. Showers and frontal rain falling through rather stable underlying atmosphere are characterized by a small value for $\lambda$, inducing insignificant pressure rises at the surface.

In-cloud precipitation does not always contribute to cold air production. However, melting snow or hail, which cools the downdraft beyond the moist-adiabat at the source, may partially contribute to the formation of the pressure nose under the active cell.

## 8. In- and sub-cloud precipitation

It has been shown theoretically in equation (22) that the amount of the sub-cloud evaporation, inside a pressure dome surrounded by a dry-adiabatic environment, is directly proportional to the total excess mass of the dome.

Analytical facts reveal (see figs. 5 and 6), on the other hand, that the total excess mass increases in proportion to the mass of the rain reaching the surface. This relation is given by

$$\Delta M = \psi(H) R_s \tag{26}$$

where $\psi(H)$ is the proportional constant which may be called *cold air production ratio*. This ratio varies for each system. Putting equations (22) and (26) together, we have

$$\frac{R_e}{R_s} = \frac{1}{9}\psi(H) = \frac{1}{9}\frac{\Delta M}{R_s} \tag{27}$$

or

$$\psi(H) = \frac{\Delta M}{R_s} = 9\frac{R_e}{R_s}. \tag{28}$$

Analytical results of eight mesoscale systems given in table 3 reveal that the *cold air production ratio* increases appreciably with the height of the associated convective cloud base. Fig. 13 shows that the rain which evaporates between the 9000-ft level and the surface is the same as the amount of rain reaching the ground.

By the use of aircraft and upper-air observation data of individual thunderstorms taken by the Thunderstorm Project, Florida and Ohio, Braham (1952) computed the total amount of in-downdraft evaporation to be 2.4 times as large as the surface rain. The author's approach is completely different from and independent of Braham's. Fig. 13 reveals, however, that Braham's estimate of the in-cloud evaporation fits in very well with the author's value.

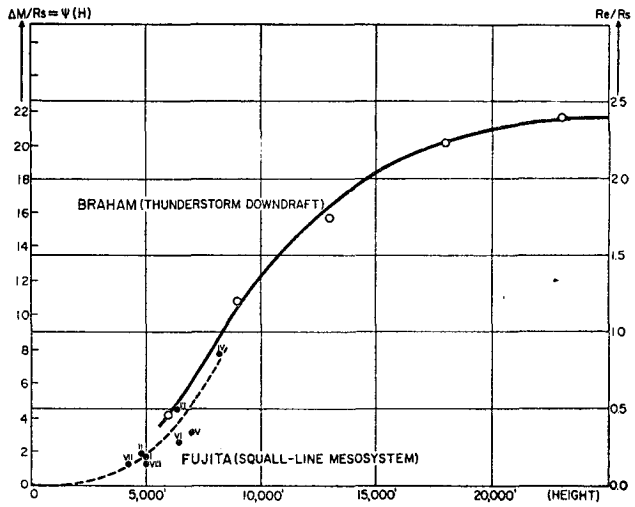


FIG. 13. Upper curve: in-cloud evaporation which Braham computed by using the water budgets of thunderstorm circulation. Lower curve: Sub-cloud evaporation obtained by Fujita with the use of total excess mass and total surface rain accompanied by squall-line mesosystems. It should be noted that the author's curve was obtained without specific knowledge of Braham's data and by a different approach.

It is a commonly observed phenomenon that squalls in a humid region are not associated with an appreciable high pressure system. On the contrary, showers over an arid land are accompanied by a tremendous high pressure dome with winds diverging from the rain areas. The reasons for these phenomena can be explained by the difference in the *cold air production ratio* which varies from 0.5 to 10.0 corresponding to a cloud base of 3000 to 9000 ft above the surface.

When the *cold air production ratio is large*, the storm is characterized by the term *thunderstorm*; when it is small, by *rainshower*.

## 9. Conclusions

It was proved in this paper that the initiation of a mesoscale pressure dome can be explained by the

TABLE 3. Statistics of eight mesoscale pressure systems occurring over the Central United States.

| System | Date | Location | Max. size | $\psi(H)$ | Cloud base | Movement |
|---|---|---|---|---|---|---|
| I | Jun 4 '53 | Ia-Wis-Mich | 300 × 500 mi | 1.7 | 5000 ft | WSW 35 kn |
| II | Jun 5 '53 | Ill-Mich | 200 × 400 | 1.9 | 4800 ft | W 30 |
| III | Jul 20 '57 | Oklahoma | 150 × 200 | 4.5 | 6300 ft | Stationary |
| IV | Jul 20 '57 | N. Texas | 400 DIA | 8.7 | 8200 ft | Stationary |
| V | Jul 20 '57 | Cent. Tex | 100 × 150 | 3.0 | 7000 ft | Stationary |
| VI | Jul 20 '57 | Cent. Tex | 200 × 400 | 2.5 | 6400 ft | Stationary |
| VII | Jul 20 '57 | Louisiana | 200 × 400 | 1.3 | 4200 ft | NNW 5 |
| VIII | Aug 13 '47 | Ohio | 20 DIA | 1.4 | 5000 ft | SSW 5 |

sub-cloud evaporation of raindrops. The term *cold air production ratio* was introduced in order to explain the fact that precipitation systems are accompanied by pressure systems of various sizes and intensities. This ratio varies from 0.5 to 10 depending upon the thermodynamical characteristics of the sub-cloud atmosphere.

The mass of the sub-cloud cold dome beneath a hurricane rainband is negligibly small since the production ratio corresponding to the cloud base in a hurricane is no more than 0.5, which is only one tenth of the value commonly observed in case of squall lines over the Midwest.

From the forecasting point of view, if isolines of *cold air production ratio* were drawn over the area of expected precipitation, a forecast of pressure systems could be made by performing a multiplication

$$R_s' \times \psi'(H)$$

where $R_s'$ and $\psi'(H)$ are respectively the forecast surface rain and *cold air production ratio* determined by the expected height of the convective cloud base.

*Acknowledgments.*—The author is very grateful to Drs. H. R. Byers and R. R. Braham, Jr. for their kind suggestions and useful comments in the completion of this paper.

## REFERENCES

Braham, R. R., Jr., 1952: The water and energy budgets of the thunderstorm and their relation to thunderstorm development. *J. Meteor.*, **9**, 227–242.

Byers, H. R., and R. R. Braham, Jr., 1949: *The thunderstorm.* U. S. Govt. Print. Off.

——, 1951: *Compendium meteor.* Boston, Amer. meteor. Soc., 681–693.

Fujita, T., 1955: Result of detailed synoptic studies of squall lines. *Tellus*, **7**, 405–436.

——, H. Newstein, and M. Tepper, 1956: *Mesoanalysis: an important scale in the analysis of weather data.* Pap. No. 39, U. S. Wea. Bur.

——, 1957: *Three-dimensional mesoanalysis of a squall line.* Res. Rep. No. 1, Illinois State Water Survey, Meteor. Lab.

——, and H. A. Brown, 1958: A study of mesosystems and their radar echoes. *Bull. Amer. meteor. Soc.*, **39**, 538–554.

——, 1959: Study of mesosystems associated with stationary radar echoes. *J. Meteor.*, **16**, 38–52.

Levine, J., 1942: The effect of vertical accelerations on pressure during thunderstorms. *Bull. Amer. meteor. Soc.*, **23**, 52–61.

Petterssen, S., 1956: *Weather analysis and forecasting*, Vol. 2. New York, N. Y., McGraw-Hill Book Co., Inc., 266 pp.

U. S. Weather Bureau, 1956: *Manual of surface observations.* Circular N, 7th Edition, p. 79.

Schaffer, W., 1947: The thunderstorm high. *Bull. Amer. meteor. Soc.*, **28**, 351–355.

Suckstorff, G. A., 1935: Die Strömungsvorgänge in Instabilitätsschauern. *Z. Meteor.*, **25**, 449–452.

Tepper, M., 1950: A proposed mechanism of squall lines: the pressure jump line. *J. Meteor.*, **7**, 21–29.

——, 1952: *The application of the hydraulic analogy to certain atmospheric flow problems.* Res. Pap. No. 35, U. S. Wea. Bur.